Histopathology of resected tissue from repair of anomalous aortic origin of a coronary artery: Potential mechanism of coronary artery compression

Chrystalle Katte Carreon, MD,[a,b] Stephen P. Sanders, MD,[a,c] Alessandra M. Ferraro, MD,[c,d] Kimberlee Gauvreau, ScD,[d,e] Meena Nathan, MD, MPH,[f,g] Shuhei Toba, MD,[a,h] Jane W. Newburger, MD, MPH,[c,d] Rebecca S. Beroukhim, MD,[c,d] and Luis G. Quinonez, MD[f,g]

ABSTRACT

Objective: This study aimed to describe the histomorphologic characteristics of resected (unroofed) common wall tissue from repair of anomalous aortic origin of a coronary artery and to determine whether the histologic features correlate with clinical and imaging findings.

Methods: The histology of resected tissue was analyzed and reviewed for the presence of fibrointimal hyperplasia, smooth muscle disarray, mucoid extracellular matrix accumulation, mural fibrosis, and elastic fiber disorganization and fragmentation using hematoxylin and eosin and special stains. Clinical, computed tomography imaging, and surgical data were correlated with the histopathologic findings.

Results: Twenty specimens from 20 patients (age range, 7-18 years; 14 males) were analyzed. Anomalous aortic origin of a coronary artery involved the right coronary in 16 (80%), and a slit-like ostium was noted in 18 (90%). By computed tomography imaging, the median proximal coronary artery eccentricity index was 0.4 (range, 0.20-0.90). The median length of intramural course was 8.2 mm (range, 2.6-15.2 mm). The anomalous vessel was determined to be interarterial in 14 patients (93%, 15 had evaluable images). The median distance from a commissure was 2.5 mm above the sinotubular junction (STJ) (range: 2 mm below the STJ–14 mm above the STJ). Prominent histopathologic findings included elastic fiber alterations, mural fibrosis, and smooth muscle disarray. The shared wall of the aorta and intramural coronary artery is more similar to the aorta histologically. Mural fibrosis and elastic fiber abnormalities tended to be more severe in patients >10 years of age at the time of surgery, but this did not reach statistical significance. The extent of vascular changes did not appear to have a clear relationship with the imaging features.

Conclusions: The findings confirm the aortic wall–like quality of the intramural segment of the coronary artery and the presence of pathologic alterations in the wall microstructure. (JTCVS Open 2023;15:412-23)

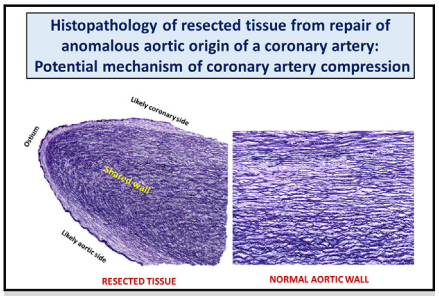

The shared wall of aorta and intramural coronary resembles the aortic microstructure.

CENTRAL MESSAGE

Our study is the first to explore the microanatomy of coronary arteries with anomalous aortic origin in living patients, which offers a histopathologic correlate for the mechanism of sudden death.

PERSPECTIVE

The shared wall between the intramural coronary segment and aorta is more like an elastic aortic wall than a muscular coronary artery wall, decreasing stiffness and increasing collapsibility. Wall abnormalities in these vessels appear to become more apparent with increasing age. These new data expand our understanding of AAOCA and may inform future treatment strategies.

From the [a]The Cardiac Registry, Departments of Cardiology, Pathology, and Cardiac Surgery, Boston Children's Hospital, Boston, Mass; [b]Department of Pathology, Harvard Medical School, Boston, Mass; [c]Department of Pediatrics, Harvard Medical School, Boston, Mass; [d]Department of Cardiology, Boston Children's Hospital, Boston, Mass; [e]Department of Biostatistics, Harvard T.H. Chan School of Public Health, Boston, Mass; [f]Department of Cardiac Surgery, Boston Children's Hospital, Boston, Mass; [g]Department of Surgery, Harvard Medical School, Boston, Mass; and [h]Department of Thoracic and Cardiovascular Surgery, Mie University Graduate School of Medicine, Mie, Japan.

This research was supported by the Kostin Family Innovation Fund, Boston Children's Hospital, Boston, MA, USA.

Received for publication Feb 23, 2023; revisions received June 21, 2023; accepted for publication July 10, 2023; available ahead of print Sept 5, 2023.

Address for reprints: Chrystalle Katte Carreon, MD, Department of Pathology, Boston Children's Hospital and Harvard Medical School, 300 Longwood Ave, Boston, MA 02215 (E-mail: Katte.Carreon@childrens.harvard.edu).

2666-2736

https://doi.org/10.1016/j.xjon.2023.07.020

Abbreviations and Acronyms
AAOCA = anomalous aortic origin of a coronary artery
CT = computed tomography

Anomalous aortic origin of a coronary artery (AAOCA) from an inappropriate sinus of Valsalva is a relatively rare congenital condition. Its known association with sudden cardiac death depicts the potential gravity of its clinical consequence.[1-5] Most commonly, the right coronary artery arises from the left coronary sinus of Valsalva and takes an interarterial course.[6] Usually, the proximal part of the anomalous coronary artery has an intramural segment coursing within the wall of the aorta before exiting the aortic adventitia. The intramural coronary artery segment shares a common media with the aorta.[7] The most common surgical procedure to treat this condition is *unroofing*, in which the intramural segment of the coronary artery is incised from within the aorta and the common wall resected until the coronary artery exits the aortic wall from within the appropriate sinus.[8-10] There are few descriptions of the pathologic characteristics of the anomalous coronary wall, and most are limited to reports of isolated cases.[4,7,11-14] This study aims to describe the histopathologic characteristics of the common wall tissue excised (unroofed) during repair of AAOCA and to determine whether histologic features correlate with clinical and imaging findings.

METHODS

Pathology

This was a retrospective review of existing pathology specimens that were obtained at the time of surgical unroofing between 2013 and 2020. The Institutional Review Board of Boston Children's Hospital approved this study (Institutional Review Board no. P00038929; approved on June 1, 2022), and all families gave consent for use of discarded tissue for research. Using the existing AAOCA and Heart Center Cardiac Registry databases, we identified those patients in whom pathologic specimens of unroofed tissue had been submitted for histopathologic evaluation. Archived routine hematoxylin-and-eosin–stained slides of unroofed tissue were reviewed for fibrointimal hyperplasia, mural smooth muscle disarray, mucoid extracellular matrix accumulation, mural fibrosis, and elastic fiber disorganization and fragmentation. The amount of fibrosis was further evaluated using Masson trichrome stain, and the morphology of elastic fibers was analyzed using Miller's elastic stain, both performed on existing paraffin-embedded tissue blocks. Immunohistochemistry for smooth muscle actin and CD31 (an endothelial cell marker) was performed on representative cases to examine vascular wall smooth muscle and endothelial cells, respectively. A semiquantitative pathologic grading scheme was used to score fibrosis, mucoid extracellular matrix accumulation, and elastic fiber disorganization and fragmentation in the unroofed tissue fragments:

Fibrointimal hyperplasia: 0—absent; 1—minimal to mild: thickening comparable with <20 fibroblast/smooth muscle cell layers or <25% of the vessel wall thickness; 2—moderate to marked: thickening comparable with >20 fibroblast/smooth muscle cell layers or >25% of the wall thickness.

Mural smooth muscle disarray and hyperplasia: 0—absent or comparable with the very mild disturbance appreciated at the junction of aorta and coronary ostium; 1—minimal to mild: <30% of tissue involvement in multiple fragments or in single-fragment specimens; 2—moderate to marked: >30% to diffuse involvement in multiple tissue fragments or in single-fragment specimens.

Mucoid extracellular matrix accumulation: 0—absent; 1—minimal to mild: scattered small discrete foci of myxoid ground substance often confined in between layers of smooth muscle cells and elastic lamellae; 2—moderate to marked: multifocal to confluent pools of myxoid substance with distinct microcyst formation.

Mural fibrosis: 0—absent or no evidence of significant wall fibrosis; 1—minimal to mild: <30% of tissue involvement in multiple fragments or in single-fragment specimens; 2—moderate to marked: >30% to diffuse involvement in multiple tissue fragments or in single-fragment specimens.

Age bracket–matched tissue sections of right and left coronary–aorta junctions from deceased subjects ages 5, 7, 8.5, 13, and 15.5 years with structurally normal hearts, and coronary arteries were obtained from the archived heart specimens in the Cardiac Registry and stained as described previously for direct comparison. In addition, aortic walls, including aortic valve commissures and cusps from age bracket-matched normal hearts, were serially sectioned from superior to inferior. The sections were used as reference to determine the microstructure of pericommissural regions compared with the vascular wall within the sinus of Valsalva.

Clinical, Computed Tomography (CT) Imaging, and Surgical Data

Basic demographic and clinical characteristics of the patient cohort were abstracted from the AAOCA database and/or the electronic medical record. Preoperative CT angiographic images were analyzed by an expert observer using Circle Cardiovascular Imaging software (cvi42 version, 5.12.1). The anomalous coronary artery was evaluated for location of origin, course (interarterial or retroaortic, and distance to a commissure), location of exit point from the aorta, angle of take-off from the aorta, and length of interarterial and intramural course. The relationship of the anomalous coronary artery to a commissure was determined by measuring the distance from a commissure and noting whether the vessel crosses the commissure. Distance from a commissure is determined by obtaining long-axis images using multiplanar reconstructed views, and the distance from the tip of the commissure to the coronary orifice was measured. Measurements were positive if the coronary was positioned above the sinotubular junction and negative if the coronary orifice was positioned below the sinotubular junction. Endoluminal views were also obtained for qualitative assessment of the relationship of the coronary to the commissure, in order to verify measurements. The anomalous coronary artery is considered to cross a commissure when the circumferentially oriented coronary artery arising from the opposite coronary sinus of Valsalva crosses the plane of the intercoronary commissure either above, at, or below the sinotubular junction. In contrast, an anomalous coronary arising from the appropriate sinus of Valsalva, above the intercoronary commissure, or a coronary artery oriented vertically (irrespective of origin) does not cross a commissure. Locations of origin and exit point were coded according to previously established methods. Dimensions of both coronaries were measured, and coronary artery dominance (right, left, or co-dominant) was assessed (Figure 1). Slit-like was defined as minor dimension ÷ major dimension of <0.5, and stenosis/narrowed ostium was defined as intraoperative dimension between 0.5 and 1 mm.

Statistical Analysis

Categorical variables were summarized with frequencies and percentages, and continuous variables were summarized with medians and ranges. Categorical characteristics were compared between groups using the Fisher

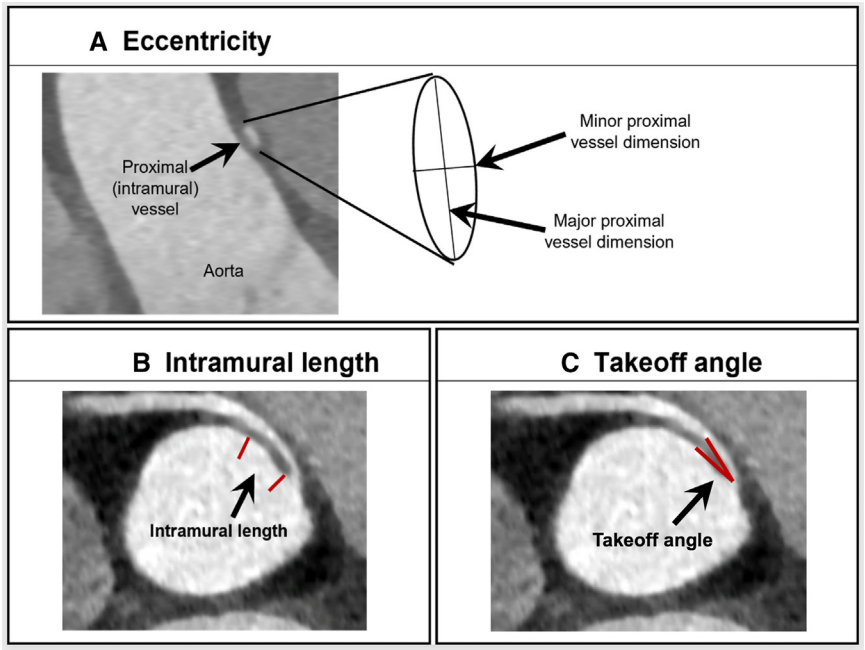

FIGURE 1. Coronary artery measurements. Eccentricity index is the minor proximal dimension ÷ major proximal dimension (A). Intramural length is the measured length of the oval segment of vessel within the wall of the aorta (B). Takeoff angle is the measured angle between the proximal coronary artery and aortic wall (C).

exact test and continuous variables using the exact Wilcoxon rank sum test. No adjustment was made for multiple comparisons in these exploratory analyses. Stata, version 16, was used for all analyses.

RESULTS

Patient Demographics, Clinical Features, and Intraoperative Findings

Twenty patients (14 males—70%) were included in the study. The median age at surgery was 12 years (range, 7-18 years). Sixteen (80%) patients were symptomatic and presented with chest pain (9) syncope (3), presyncopal episodes (2), ventricular dysrhythmias (1), and dizziness with "intestinal angina" (1). The remaining 4 patients were incidentally diagnosed, including 1 incidentally discovered at the time of radiofrequency ablation of an accessory pathway at an outside hospital and another during evaluation of a murmur secondary to a large secundum-type atrial septal defect. External dysmorphic features were noted in 2 patients: absent ears in one and pectus excavatum and scoliosis in the other.

Intraoperatively, the AAOCA diagnoses were anomalous right coronary artery in 16 (80%) and anomalous left coronary artery in 4 (20%). Of the 16 anomalous right coronary artery cases, 13 were from the left sinus of Valsalva (one of which being the left-sided sinus in a bicommisural aortic valve), 2 from above the right sinus of Valsalva, and 1 from above the intercoronary commissure. Of the 4 anomalous left coronary artery cases, 3 were from the right sinus of Valsalva and 1 was from the top of the left-noncoronary commissure.

The preoperative CT angiography AAOCA diagnoses were confirmed intraoperatively. By direct inspection, a slit-like ostium was observed in 18 (90%) patients, a narrowed ostium in 1 (5%), and the ostium was not described in 1 (5%). Surgical unroofing was performed in all cases with excision of the common wall, resulting in widening of the ostium. Excision of the common wall for the entire length of the intramural segment ensured an unobstructed ostium with laminar blood flow documented on postoperative imaging.

Of note, 3 (15%) patients were noted to have yellow discoloration/possible fatty streaks, mostly mild, involving the aortic or coronary artery wall: one in the ascending aorta, one in the sinotubular junction, and one within the intramural segment opposite the unroofed tissue. The excised or unroofed tissue did not include these foci.

CT and Intraoperative Findings

CT angiography images were available for 18 patients, 15 (83%) with anomalous origin of right coronary artery and 3 (17%) with anomalous origin of the left coronary artery. The right and left coronary arteries arose from the same sinus in 14 (77.8%) with the following relationships observed between the right and left orifices: 2 contiguous orifices adjacent to each other (9/14, 64.3%) and 5 separate noncontiguous orifices (5/14, 35.7%). All were acutely angulated to the aortic wall. The right and left coronary arteries did not arise from the same sinus in 4 cases. The coronary orifice was noted to be above the sinotubular

TABLE 1. CT angiography features of AAOCA (N = 18)

CT angiography feature	Value
Proximal coronary minor dimension, mm	1.2 (0.6-2.6)
Proximal coronary major dimension, mm	2.2 (1.7-6.5)
Proximal eccentricity*	0.4 (0.20-0.90)
Length of intramural course, mm	8.2 (2.6-15.2)
Course (n = 15)	
Interarterial	14 (93%)
Retroaortic	1 (7%)
Distance from a commissure, mm†	2.5 (−2.0 to 14)
Crosses a commissure	12 (66.7%)

Values shown are frequency (%) for categorical variables and median (range) for continuous variables. *CT*, Computed tomography. *Eccentricity = minor dimension ÷ major dimension. †A negative value indicates the orifice location to be below the sinotubular junction. Conversely, a positive value indicates the orifice location to be above the sinotubular junction.

junction in 13 cases, below the sinotubular junction in 1 case, and at the level of the sinotubular junction in 4. It crossed the intercoronary commissure in 12 cases and did not cross the commissure in 6 cases, with one originating directly above the intercoronary commissure. The CT findings regarding coronary origin, course, size, and relationship to commissure are shown in Table 1 and Table E1.

Pathology

One specimen from each of the 20 patients was analyzed. The specimens consisted of 2 to multiple minute fragments of tissue (0.1-0.5 cm) without markers for orientation. Severity of histologic features is listed in Table 2, with representative photomicrographs shown in Figure 2, *B-E*; Normal aortic wall sections (Figure 2, *A*) are shown for comparison. Intimal hyperplasia was absent or mild in all cases. Moderate-to-marked abnormalities of other vessel wall components, including smooth muscle disarray and elastic fiber disorganization (Figure 2, *B*) and fragmentation (Figure 2, *C*), were present in most specimens. On cross-tabulation, the pathologic features that tended to cluster together were elastic fiber disorganization (Figure 2, *B*), elastic fiber fragmentation (Figure 2, *C*), and mural fibrosis (Figure 2, *D*). Mucoid extracellular matrix accumulation was also frequently observed (Figure 2, *E*).

In 12 specimens, one tissue fragment had an endothelial surface on both sides with an oval edge at one end consistent with the excised common wall shared by the aorta and anomalous coronary artery, with the smooth oval end representing a portion of the coronary ostium (Figure 2, *F*), which occasionally exhibited mild fibrointimal hyperplasia (Figure 2, *G*). The architecture of the shared wall, apparent in the 12 specimens where this was intact, consisted of a bilayer band of elastic fibers and smooth muscle cells/myofibroblasts. The outermost (subendothelial) layer ran parallel to the long axis of the tissue fragment along the aortic side, curving around the ostial end to continue along the coronary side. The deep layer appears to run somewhat perpendicular to this outermost layer (Figure 2, *F*). Immunohistochemistry for CD31 confirmed endothelium along the intimal surface. Smooth muscle actin highlights myofibroblasts.

Histology of Normal Specimens

In the 5 normal hearts, we observed mild intimal hyperplasia, smooth muscle disarray, and disturbance in the elastic fiber orientation with some degree of fragmentation at the normal coronary artery–aorta junction. We noted similar findings near an aortic valve commissure and for a distance of 3 to 4 mm above the commissure with accentuation of collagen fibers surrounding the cusp attachment points. In contrast, the vascular walls within the sinuses of Valsalva showed relatively well-aligned and intact elastic fibers and smooth muscle. These findings were qualitatively similar to those in the AAOCA specimens but quantitatively much less marked.

Clinical–Pathologic Correlation

Mural fibrosis, elastic fiber disorganization, and elastic fiber fragmentation tended to be more severe in patients >10 years of age at the time of surgery, but this did not reach statistical significance (Table E2). The extent of vascular pathologic changes did not appear to have a clear relationship with CT angiogram features, possibly due to the small number of subjects (Table E3). All findings are summarized in Table E1.

DISCUSSION

Although the macroscopic anatomy of coronary arteries with anomalous aortic origin is understood, little is known

TABLE 2. Severity of histopathologic features of resected tissue from AAOCA (N = 20)

Histopathologic feature	Absent	Minimal-mild	Moderate-marked
Fibrointimal hyperplasia	11 (55%)	9 (45%)	0
Smooth muscle proliferation/disarray	1 (5%)	7 (35%)	12 (60%)
Mucoid extracellular matrix accumulation	1 (5%)	10 (50%)	9 (45%)
Mural fibrosis	1 (5%)	7 (35%)	12 (60%)
Elastic fiber disorganization	0	4 (20%)	16 (80%)
Elastic fiber fragmentation	1 (5%)	5 (25%)	14 (70%)

Values shown are number (%).

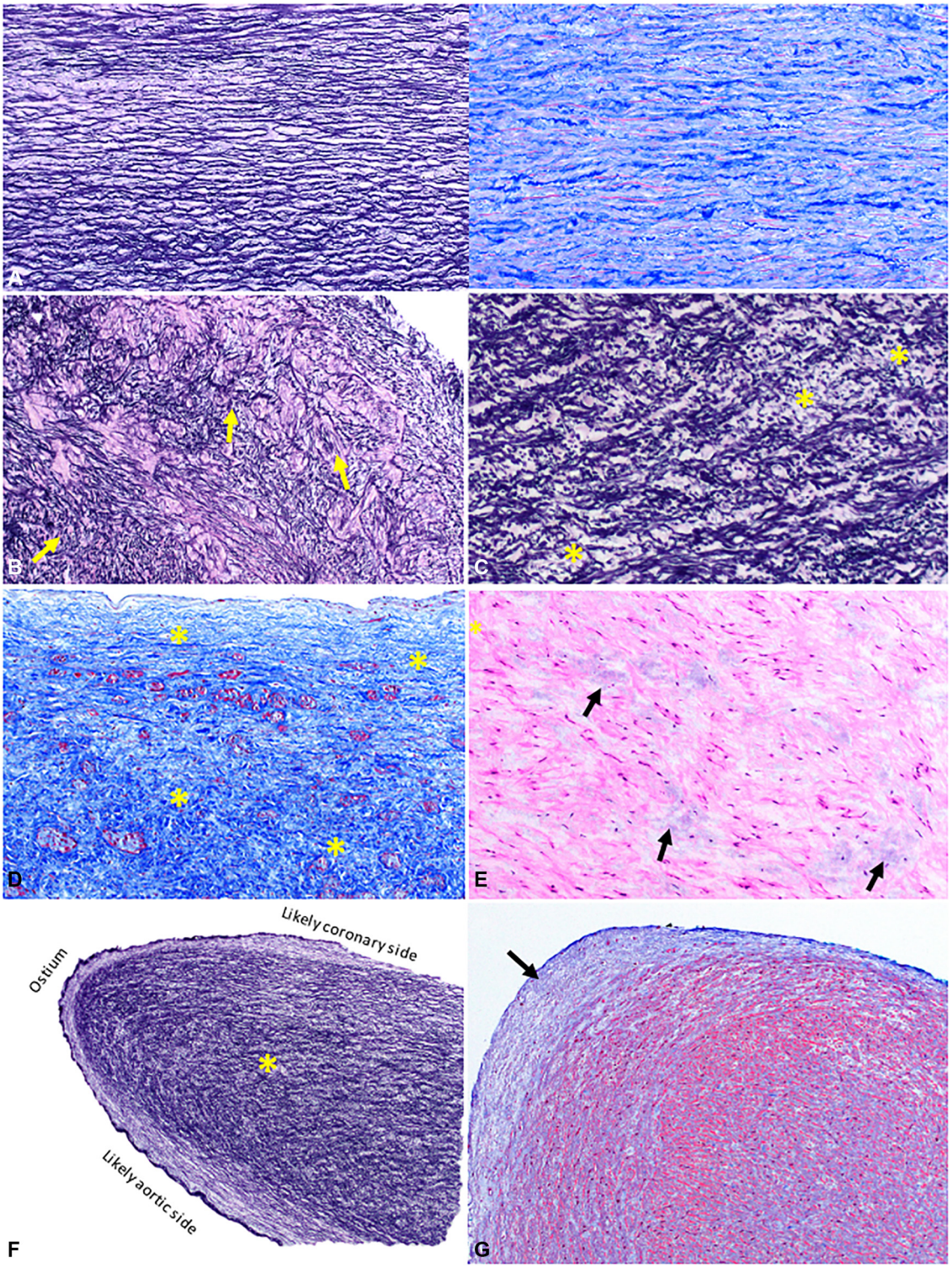

FIGURE 2. The most commonly observed histopathologic changes in unroofed coronary tissue. For reference, a section of proximal ascending aorta just before its junction with the coronary ostium of a normal heart from a 15-year-old patient is shown (A) to highlight the orderly orientation of elastic fibers (*left panel*, elastic stain), and collagen and fibroblasts/myofibroblasts (*right panel*, trichrome stain). The same uniform orientation is seen in the aorta from all representative normal tissues from different age groups. Elastic fiber disorganization or loss of the organized parallel arrangement (B) and fragmentation (*) (C) are the 2 most common findings. Mural fibrosis (*blue area* highlighted by trichrome stain and marked by *yellow asterisks*) (D) and mucoid extracellular matrix accumulation (*arrows*) (E) are also observed. The shared wall (*) (F) of the aorta and intramural coronary artery is more similar to the microstructure of the aorta. It is covered by a continuous endothelium-lined surface that occasionally exhibits mild intimal hyperplasia (*blue region* pointed by an *arrow*) at the tip (G).

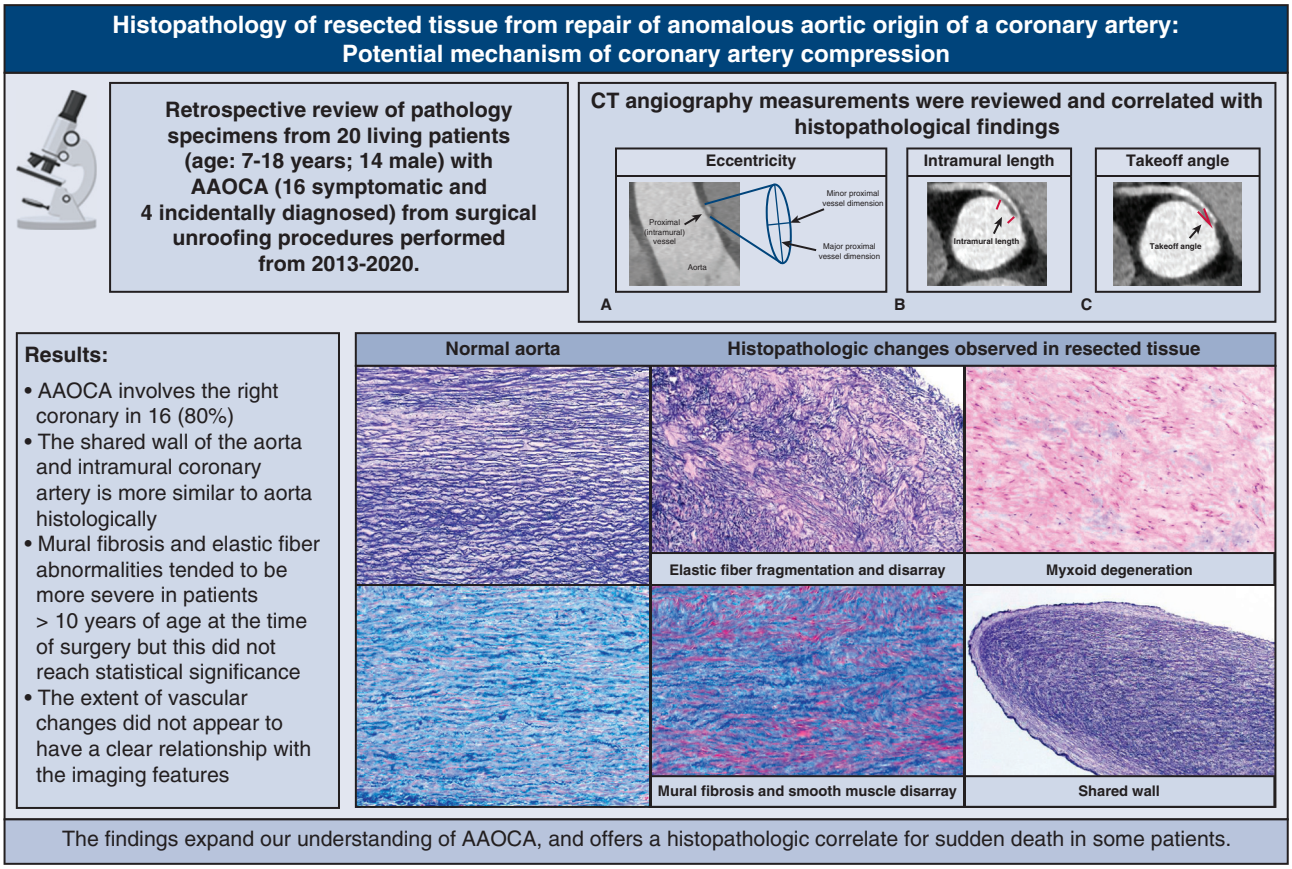

FIGURE 3. The histopathologic findings observed in resected tissue from repair of anomalous aortic origin of a coronary artery offers a plausible mechanism of coronary compression in these patients. *CT*, Computed tomography; *AAOCA*, anomalous aortic origin of a coronary artery.

about the histology of these aberrant vessels. We sought to determine whether the microscopic anatomy could provide insights into the pathophysiology that leads to ischemic symptoms and sudden death. Previous reports were derived mostly from postmortem studies and reports of coronary findings in isolated cases of sudden death.[4,7,11-16] Most involve older patients with superimposed coronary artery disease.[12,14] One case report described abundant elastic fibers with little smooth muscle in the intra-arterial segment of an AAOCA in a child who died suddenly.[4]

The availability of the excised vascular wall tissue in our institution for pathologic evaluation following surgical unroofing enabled us to closely examine the walls of these maldeveloped vessels at the cellular level for the first time in a cohort of living pediatric patients. We discovered varying degrees of wall fibrosis, smooth muscle disarray and hyperplasia, elastic fiber disorganization and fragmentation, and extracellular mucoid matrix accumulation in the resected common wall, with the elastic fiber alterations being the most frequent finding. Curiously, fibrointimal hyperplasia was not a prominent characteristic in these excised vascular wall fragments. Rather, the most dramatic changes observed were in the tunica media involving the elastic fiber morphology. We considered that these findings could be secondary to the close proximity of the excised segment to a commissure, given the histologic pattern observed in pericommissural areas in the vessel walls of the normal heart. However, the findings in most of the AAOCA cases were much more marked than what we observed in normal vessels. In addition, in 1 recent case that was not included in the period of study, in which the origins of excised tissues were known—one being far from and one being close to a commissure—similar features were observed, revealing that the aforementioned changes can also be observed in areas well away from the commissures.

In a subset of our cases, the intact common wall with a portion of the coronary ostium, a double-sided endothelium-lined tissue fragment, was submitted. We confirmed previous case reports of a common medial layer shared by the aorta and the intramural segment of the anomalous coronary artery without any intervening adventitial layer.[4,7,11,13] In addition, we observed that the shared wall resembles the histomorphologic composition of the aorta more than the coronary artery, harboring abundant (and often abnormal) elastic fibers and a lesser amount of medial

smooth muscle than usual, similar to a previous case report.[4] The abundant elastic fibers confer resilience and increased flexibility to the normal aortic wall.[17] In contrast, muscular arteries, such as the coronary arteries, have been found to be more rigid than elastic arteries,[18-20] owing to their more muscularized wall with fewer elastic fibers. This altered microstructure of the coronary wall may render these anomalous vessels more vulnerable to compression during systolic expansion of the aorta, particularly during physical exertion, when cardiac output and blood pressure are elevated.[1,21] The absence of significant intimal changes speaks against increased shear stress, leading to intimal reaction as a cause of luminal narrowing. Rather, the structural wall abnormalities that render the vessel more susceptible to compression favor intermittent functional deformation of the coronary artery as the most likely mechanism for inducing ischemia. In addition, physiologic changes in vascular smooth muscle in response to various stimuli are responsible for the vasodilation and vasoconstriction observed in normal coronary arteries.[22,23] Of note, in a separate analysis of CT angiograms of AAOCA, we have demonstrated a relative lack of vasodilation in the proximal intramural segments of AAOCA vessels compared with the distal nonintramural segments.[24] The structure of the wall of these intramural vessels (elastic rather than muscular) may explain the lack of vasodilation and hence provide additional mechanistic insight into the pathogenesis of exertional ischemia and sudden death. Overall, it is possible that the medial changes discovered were congenital, related to the abnormally formed vessels/vessel wall that may get worse over time due to a number of factors (eg, abnormal wall microstructure, hemodynamics).

A complex signaling mechanism directs the developing peritruncal vascular plexus to anastomose with the aorta at the appropriate sites in the aortic wall to establish a stable coronary system.[25,26] So far, 3 different cell types have been identified to participate in this process: *epicardium-derived cells*, which regulate apoptosis in the peritruncal region to facilitate attachment of developing coronaries to the aorta; *preotic neural crest cells*, which have been shown to influence coronary stem (coronary–aorta connections) and orifice formation; and *intra-aortic cardiomyocytes* at stem sites, which are thought to influence normal development and placement of coronary stems.[26] Although the exact mechanism in humans is yet to be fully elucidated, perturbation of these highly orchestrated pathways has been demonstrated to result in aberrant coronary orifice morphology and location in animal models.[26,27] The observed wall microstructure of the intramural segment of the coronary artery—being more reminiscent of an elastic arterial wall—likewise suggests erroneous development and penetration of the peritruncal coronary plexus into an already-established aortic wall.

The excised lip of the ostium often showed mild fibrointimal hyperplasia, which is slightly more prominent over the tip and along the coronary artery side. Given that the ostium was usually described as slit-like, it is conceivable that even mild fibrointimal hyperplasia could contribute to further narrowing of the ostium and restriction of blood flow.

We did not find a clear association between the pathologic changes in the vascular wall fragments and clinical or imaging features. This could be due to the small sample size as well as the small tissue fragments without orientation marks available for analysis. Nevertheless, the current investigation is the first to explore the microanatomy of these anomalous coronary arteries in a cohort of living patients.

Limitations

The limitations of our study include a relatively small sample size and the lack of orientation of the excised vascular wall fragments.

CONCLUSIONS

These findings add to the scarce histopathologic data on AAOCA and suggest that there are inherent structural abnormalities of the walls of these vessels. The shared wall of the intramural segment is more akin to an altered elastic aortic wall than to a muscular coronary artery wall, a plausible histopathologic correlate for the proposed increased coronary compressibility mechanism for sudden cardiac death in the affected patients. The abnormalities in the wall microstructure of the intramural segments of these anomalous coronary arteries, which may be compounded by secondary changes acquired over time, are reasonable indications for surgical repair. The new information expands our understanding of AAOCA and may inform future treatment strategies for these patients (Figure 3).

Conflict of Interest Statement

The authors reported no conflicts of interest.

The *Journal* policy requires editors and reviewers to disclose conflicts of interest and to decline handling or reviewing manuscripts for which they may have a conflict of interest. The editors and reviewers of this article have no conflicts of interest.

References

1. Finocchiaro G, Behr ER, Tanzarella G, Papadakis M, Malhotra A, Dhutia H, et al. Anomalous coronary artery origin and sudden cardiac death: clinical and pathological insights from a national pathology registry. *JACC Clin Electrophysiol*. 2019;5:516-22.
2. Deng ES, O'Brien SE, Fynn-Thompson F, Chen MH. Déjà vu: recurrent sudden cardiac arrests in a child with an anomalous left coronary artery. *JACC Case Rep*. 2021;3:1527-30.
3. Campiche DE, Vallée JP, Carballo D. High risk features of an anomalous origin of the right coronary artery. *Case Rep Cardiol*. 2021;2021:1649723.
4. Sakai K, Saito K, Takada A, Suzuki H. Unexpected death in a young child associated with anomalous aortic origin of the left main coronary artery without

physical exertion: a case of an anomalous coronary artery with highly abundant elastic fibers. *Leg Med*. 2021;53:101965.
5. Jo Y, Uranaka Y, Iwaki H, Matsumoto J, Koura T, Negishi K. Sudden cardiac arrest: associated with anomalous origin of the right coronary artery from the left main coronary artery. *Tex Heart Inst J*. 2011;38:539-43.
6. Poynter JA, Bondarenko I, Austin EH, DeCampli WM, Jacobs JP, Ziemer G, et al; Congenital Heart Surgeons' Society AAOCA Working Group. Repair of anomalous aortic origin of a coronary artery in 113 patients: a Congenital Heart Surgeons' Society report. *World J Pediatr Congenit Heart Surg*. 2014; 5:507-14.
7. Basso C, Maron BJ, Corrado D, Thiene G. Clinical profile of congenital coronary artery anomalies with origin from the wrong aortic sinus leading to sudden death in young competitive athletes. *J Am Coll Cardiol*. 2000;35: 1493-501.
8. Fedoruk LM, Kern JA, Peeler BB, Kron IL. Anomalous origin of the right coronary artery: right internal thoracic artery to right coronary artery bypass is not the answer. *J Thorac Cardiovasc Surg*. 2007;133:456-60.
9. Davies JE, Burkhart HM, Dearani JA, Suri RM, Phillips SD, Warnes CA, et al. Surgical management of anomalous aortic origin of a coronary artery. *Ann Thorac Surg*. 2009;88:844-7; discussion 847-8.
10. Romp RL, Herlong JR, Landolfo CK, Sanders SP, Miller CE, Ungerleider RM, et al. Outcome of unroofing procedure for repair of anomalous aortic origin of left or right coronary artery. *Ann Thorac Surg*. 2003;76:589-95; discussion 595-6.
11. Frescura C, Basso C, Thiene G, Corrado D, Pennelli T, Angelini A, et al. Anomalous origin of coronary arteries and risk of sudden death: a study based on an autopsy population of congenital heart disease. *Hum Pathol*. 1998;29: 689-95.
12. Hata Y, Kinoshita K, Kudo K, Ikeda N, Nishida N. Anomalous origin of the right coronary artery from the left coronary sinus with an intramural course: comparison between sudden-death and non-sudden-death cases. *Cardiovasc Pathol*. 2015;24:154-9.
13. Tavora F, Li L, Burke A. Sudden coronary death in children. *Cardiovasc Pathol*. 2010;19:336-9.
14. Iino M, Kimura T, Abiru H, Kaszynski RH, Yuan QH, Tsuruyama T, et al. Unexpected sudden death resulting from anomalous origin of the right coronary artery from the left sinus of Valsalva: a case report involving identical twins. *Leg Med*. 2007;9:25-9.
15. Lalu K, Karhunen PJ, Rautiainen P. Sudden and unexpected death of a 6-month-old baby with silent heart failure due to anomalous origin of the left coronary artery from the pulmonary artery. *Am J Forensic Med Pathol*. 1992;13:196-8.
16. Taylor AJ, Rogan KM, Virmani R. Sudden cardiac death associated with isolated congenital coronary artery anomalies. *J Am Coll Cardiol*. 1992;20:640-7.
17. Midwood KS, Schwarzbauer JE. Elastic fibers: building bridges between cells and their matrix. *Curr Biol*. 2002;12:R279-81.
18. Kohn JC, Lampi MC, Reinhart-King CA. Age-related vascular stiffening: causes and consequences. *Front Genet*. 2015;6:112.
19. Ebrahimi AP. Mechanical properties of normal and diseased cerebrovascular system. *J Vasc Interv Neurol*. 2009;2:155-62.
20. Akhtar R, Sherratt MJ, Cruickshank JK, Derby B. Characterizing the elastic properties of tissues. *Mater Today*. 2011;14:96-105.
21. Angelini P. Anomalous origin of the left coronary artery from the opposite sinus of Valsalva: typical and atypical features. *Tex Heart Inst J*. 2009;36:313-5.
22. Zhuge Y, Zhang J, Qian F, Wen Z, Niu C, Xu K, et al. Role of smooth muscle cells in cardiovascular disease. *Int J Biol Sci*. 2020;16:2741-51.
23. Maruhashi T, Kajikawa M, Nakashima A, Iwamoto Y, Iwamoto A, Oda N, et al. Nitroglycerine-induced vasodilation in coronary and brachial arteries in patients with suspected coronary artery disease. *Int J Cardiol*. 2016;219:312-6.
24. Ferraro AM, Uslenghi A, Lu M, Newburger JW, Nathan M, Quinonez LG, et al. Computed tomography angiography (CTA) of anomalous aortic origin of a coronary artery (AAOCA): which measurements are accurate and reliable? *J Cardiovasc Comput Tomogr*. 2023;17:130-7.
25. Sharma B, Chang A, Red-Horse K. Coronary artery development: progenitor cells and differentiation pathways. *Annu Rev Physiol*. 2017;79:1-19.
26. Tian X, Pu WT, Zhou B. Cellular origin and developmental program of coronary angiogenesis. *Circ Res*. 2015;116:515-30.
27. Arima Y, Miyagawa-Tomita S, Maeda K, Asai R, Seya D, Minoux M, et al. Preotic neural crest cells contribute to coronary artery smooth muscle involving endothelin signalling. *Nat Commun*. 2012;3:1267.

Key Words: anomalous aortic origin of coronary artery, anomalous coronary, sudden cardiac death, coronary artery stenosis, coronary artery compression, coronary artery histopathology

TABLE E1. Clinical, pathologic, and CT findings in all patients

Clinical findings			Pathologic findings					
Case no.	Age at surgery (y) and sex	Presentation/symptoms	Fibrointimal hyperplasia	Mural smooth muscle disarray and hyperplasia	Mucoid extracellular matrix accumulation	Mural fibrosis	Fiber disorganization	Fiber fragmentation
1	9 M	Syncope on several occasions	Absent	Moderate	Minimal	Minimal	Moderate	Minimal
2	15 M	Chest pain and syncopal attacks	Absent	Moderate	Minimal	Moderate	Moderate	Minimal
3	17 M	Ventricular dysrhythmias	Absent	Moderate	Minimal	Minimal	Moderate	Moderate
4	15 F	Syncope	Minimal	Moderate	Marked	Minimal	Moderate	Marked
5	9 M	Chest pain	Absent	Marked	Minimal	Moderate	Marked	Marked
6	11 M	Presyncopal episodes	Minimal	Minimal	Minimal	Minimal	Moderate	Moderate
7	9 F	Asymptomatic, incidentally diagnosed on echo workup following adoption	Minimal	Moderate	Minimal	Minimal	Moderate	Marked
8	7 M	Chest pain during a soccer game	Absent	Minimal	Minimal	Moderate	Minimal	Moderate
9	18 M	Chest pain on exertion	Absent	Moderate	Moderate	Marked	Moderate	Minimal
10	13 M	Chest pain on exertion	Absent	Minimal	Moderate	Marked	Marked	Moderate
11	8 M	Asymptomatic; patient is known to have this condition since infancy	Absent	Absent	Absent	Minimal	Minimal	Minimal
12	12 F	Chest pain on exertion	Minimal	Moderate	Marked	Minimal	Moderate	Moderate
13	12 M	Presyncopal episodes	Absent	Moderate	Marked	Marked	Marked	Moderate
14	9 M	Dizziness and “intestinal angina”	Minimal	Moderate	Marked	Moderate	Moderate	Moderate
15	10 M	Chest pain	Minimal	Minimal	Moderate	Moderate	Marked	Moderate
16	15 F	Incidentally discovered at the time of echo for murmur secondary to a large ASD	Absent	Moderate	Minimal	Marked	Marked	Moderate
17	13 M	Incidentally diagnosed when evaluated for pectus excavatum and scoliosis	Minimal	Minimal	Moderate	Minimal	Minimal	Minimal
18	17 M	Incidentally discovered at the time of radiofrequency ablation of his accessory pathway	Minimal	Minimal	Moderate	Moderate	Minimal	Minimal
19	7 F	Chest pain, recurrent	Minimal	Minimal	Minimal	Absent	Minimal	Absent
20	14 F	Chest pain after a 5-kilometer run	Minimal	Moderate	Minimal	Moderate	Moderate	Moderate

(Continued)

TABLE E1. Continued

	Intraoperative findings			CT measurements				
Case no.	Coronary artery with anomalous origin by direct inspection	Coronary ostium morphology	Intramural course	CT length of presumed intramural course, mm	Coronary artery with anomalous origin	Sinus of origin	Relationship between right and left ostia (same sinus)	Take-off angle, degrees
1	LCA	Slit-like	N	Not available	Not available	Not available	Not available	Not available
2	RCA	Narrowed	Y, unspecified length	11.1	RCA	Left	Two contiguous orifices adjacent to each other	9.9
3	RCA	Slit-like	Y, 10-11.5 mm	15.2	RCA	Left-sided sinus*	Two separate noncontiguous	11.8
4	RCA	Slit-like	Y, unspecified length	11.8	RCA	Left	Two contiguous orifices adjacent to each other	16.1
5	RCA	Slit-like	Y, unspecified length	12.2	RCA	Above right sinus	Not applicable	12.6
6	LCA	Slit-like	Y, 8 mm	10.3	LCA	Right	Two separate noncontiguous	9.1
7	RCA	Not mentioned	Y, 3 mm	4.7	RCA	Above left sinus	Two separate noncontiguous	18.7
8	RCA	Slit-like	Y, unspecified length	2.6	RCA	Left	Two contiguous orifices adjacent to each other	13.2
9	RCA	Slit-like	Y, unspecified length	Not available	Not available	Not available	Not available	Not available
10	RCA	Slit-like	Y, unspecified length	8.6	RCA	Above left sinus	Two separate noncontiguous	12.1
11	RCA	Slit-like	Y, 8 mm	5.3	RCA	Left	Two contiguous orifices adjacent to each other	13.9
12	RCA	Slit-like	Y, 10 mm	9.7	RCA	Above intercoronary commissure	Not applicable	15.1
13	RCA	Slit-like	Y, 8 mm	6.4	RCA	Left	Two contiguous orifices adjacent to each other	18,7
14	LCA	Slit-like	Y, 6-7 mm	7.7	LCA	Top of left noncoronary commissure with minimal extension to left sinus	Not applicable	18.4
15	RCA	Slit-like	Y, 3.5 mm	4.6	RCA	Left	Two contiguous orifices adjacent to each other	17.3
16	RCA	Slit-like	Y, 2 mm	3.6	RCA	Left	Two separate noncontiguous	15
17	LCA	Slit-like	Y, unspecified length short	3	LCA	Right	Two contiguous orifices adjacent to each other	20.4
18	RCA	Very narrowed	Y, unspecified length	11.9	RCA	Left	Two contiguous orifices adjacent to each other	15.8
19	RCA	Slit-like	Y, 7 mm	7.3	RCA	Left	Two contiguous orifices adjacent to each other	16.2
20	RCA	Slit-like	Y, 9-11 mm	13.2	RCA	Above right sinus	Not applicable	8.5

(Continued)

TABLE E1. Continued

	CT measurements				
Case no.	CT proximal coronary minor dimension, mm	CT proximal coronary eccentricity index	Coronary artery course	Distance from commissure, mm	Crosses an ICC?
1	Not available	Not available	Not available	Not available	Not available
2	0.8	0.27	Interarterial	0	Crosses ICC
3	1.9	0.90	Unable to evaluate	3	Does not cross ICC
4	0.7	0.41	Interarterial	3	Crosses ICC
5	0.6	0.30	Interarterial	4	Does not cross ICC
6	1.4	0.35	Interarterial	−2†	Crosses ICC
7	0.7	0.33	Interarterial	4	Origin above ICC
8	1	0.43	Unable to evaluate	3	Crosses ICC
9	Not available	Not available	Not available	Not available	Not available
10	0.8	0.38	Interarterial	3	Crosses ICC
11	0.9	0.47	Interarterial	4	Crosses ICC
12	1.3	0.41	Interarterial	4	Does not cross ICC
13	1.5	0.43	Interarterial	0	Crosses ICC
14	1.1	0.58	Retroaortic (posterior to aortic root)	2	Does not cross ICC
15	0.9	0.47	Interarterial	0	Crosses ICC
16	1.8	0.40	Interarterial	0	Crosses ICC
17	2.6	0.63	Interarterial	2	Crosses ICC
18	1.2	0.29	Interarterial	2	Crosses ICC
19	1.2	0.60	Interarterial	3	Crosses ICC
20	1.3	0.20	Unable to evaluate	14	Does not cross ICC

CT, Computed tomography; *M*, male; *F*, female; *ASD*, atrial septal defect; *LCA*, left coronary artery; *N*, no; *RCA*, right coronary artery; *Y*, yes; *ICC*, intercoronary commissure.
*Bicommissural aortic valve with anterior–posterior directed-commissures and left- and right-sided sinuses. Both coronary orifices were in or above the left-sided sinus.
†Negative value = below the sinotubular junction.

TABLE E2. Comparison of histopathologic features by age at surgery (N = 20)

Histopathologic feature	Age at surgery	
	<10 y (n = 6)	≥10 y (n = 14)
Mural fibrosis moderate/marked	2 (33%)	10 (71%)
Fiber disorganization moderate/marked	3 (50%)	13 (93%)
Fiber fragmentation moderate/marked	3 (50%)	11 (79%)

TABLE E3. Relationship between CT angiography measurements and histopathologic findings (N = 18)

CT angiogram feature	Mural fibrosis			Fiber disorganization			Fiber fragmentation		
	Absent/ minimal (n = 7)	Moderate/ marked (n = 11)	*P* value	Absent/ minimal (n = 4)	Moderate/ marked (n = 14)	*P* value	Absent/ minimal (n = 4)	Moderate/ marked (n = 14)	*P* value
Proximal minor dimension, mm	1.20 (0.70, 1.90)	1.10 (0.60, 2.60)	.96	1.10 (0.90, 1.20)	1.20 (0.60, 2.60)	.83	1.05 (0.80, 1.20)	1.20 (0.60, 2.60)	.56
Proximal major dimension, mm	2.10 (1.70, 4.00)	3.00 (1.90, 6.50)	.19	2.15 (1.90, 4.10)	2.55 (1.70, 6.50)	.71	2.50 (1.90, 4.10)	2.20 (1.70, 6.50)	.79
Proximal eccentricity*	0.41 (0.33, 0.90)	0.40 (0.20, 0.63)	.34	0.45 (0.29, 0.60)	0.40 (0.20, 0.90)	.52	0.38 (0.27, 0.60)	0.41 (0.20, 0.90)	.75
Distal eccentricity	0.83 (0.68, 0.93)	0.79 (0.53, 0.97)	.53	0.76 (0.53, 0.93)	0.83 (0.59, 0.97)	.49	0.76 (0.65, 0.93)	0.83 (0.53, 0.97)	.71
Length of intramural course	9.70 (4.70, 15.2)	7.70 (2.60, 13.2)	.53	6.30 (2.60, 11.9)	9.15 (3.00, 15.2)	.43	9.20 (5.30, 11.9)	8.15 (2.60, 15.2)	.71
Take-off angle	15.1 (9.1, 18.7)	15.0 (8.50, 20.4)	.96	14.9 (13.2, 16.2)	15.1 (8.50, 20.4)	.96	14.9 (9.90, 16.2)	15.1 (8.50, 20.4)	.79
Distance from commissure, mm	3 (−2, 4)	2 (0, 14)	.21	3 (2, 4)	2.5 (−2, 14)	.51	2.5 (0, 4)	3 (−2, 14)	.96
Crosses an intercoronary commissure	4 (57%)	8 (73%)	.63	4 (100%)	8 (57%)	.25	4 (100%)	8 (57%)	.25

Values shown are frequency (%) for categorical variables and median (range) for continuous variables. *CT*, Computed tomography. *Eccentricity = minor dimension ÷ major dimension.